Ignition of Low-Metamorphized Coal with Continuous Lasers at Wavelengths 450 nm and 808 nm

B.P. Aduev[1]*, G.M. Belokurov[1], I.Yu. Liskov[1], D.R. Nurmukhametov[1], Z.R. Ismagilov[1,2]

[1]Federal Research Center of Coal and Coal Chemistry of Siberian Branch of the Russian Academy of Sciences,
18, Sovetsky pr., Kemerovo, Russia
[2]Boreskov Institute of Catalysis, Siberian Branch of the Russian Academy of Sciences,
5, Lavrent'ev ave., Novosibirsk, Russia

Article info	Abstract
	The paper presents the results of a comparative investigation into the kinetic and energy characteristics of the ignition of microparticles of low-metamorphized coal ranks (lignite coal and high volatile C bituminous coal) under the impact of laser radiation at the wavelengths $\lambda = 450$ nm and $\lambda = 808$ nm with an exposure time of 1 sec. Coal ignition is carried out only during irradiation. There is no transition to stationary combustion. The ignition delay time decreases monotonically with increasing radiation power density. It is established that the energy costs of ignition of the studied coal ranks may be made more economical by using laser radiation with a wavelength of $\lambda = 450$ nm. It is concluded from the results of measuring the energy characteristics of coal ignition that the absorption of radiation has a quantum nature. Two components contribute to the coal particles emission spectra measured at the initial stage of ignition: CO (CO_2^*) flame and thermal glow associated with emitted carbon particles heated to $T > 2000$ K for both coal ranks. At subsequent stages, only the glow of heated carbon particles with the thermal spectrum at $T \sim 2000$ K is observed in the spectra.

1. Introduction

Pulverized coal fuel is usually ignited in industrial furnaces with the help of fuel oil burners. The use of fuel oil causes accelerated corrosion of fuel boiler structures and environmental damage [1]. For this reason, the development of the physical methods of pulverized coal ignition is an urgent problem.

Attempts to solve this problem are at the initial stage. The first attempts at the technological solution have been already made with the help of plasmatrons [2, 3]. Pulverized coal ignition with laser radiation is a very promising method. At present, works aimed at the studies of kinetic and energy characteristics of pulverized coal ignition with the help of pulsed neodymium and continuous CO_2-lasers are carried out [4–10].

*Corresponding author.
E-mail: lesinko-iuxm@yandex.ru

Recently in our works, we have been investigating the mechanism of coal ignition under the action of the pulses of neodymium laser ($\lambda = 1064$ nm) with pulse duration $\tau_i = 120$ μs. It has been established that, depending on the energy density of laser pulses, the processes differing from each other in the kinetic and spectral characteristics may be distinguished during the ignition of coal microparticles [11–19]. In particular, when the critical energy density $H_{cr}^{(1)}$ is achieved, ignition of torches several micrometers in size is observed on the surface of coal particles. The duration of combustion at this stage coincides with the duration of the laser pulse, flame height is ~ 1 mm, and the spectrum is mainly due to CO flame glow. With an increase in energy density to a definite value $H_{cr}^{(2)} > H_{cr}^{(1)}$, specific for each studied coal rank, initiation of chemical reactions occurs in the volume of coal particles within the time interval of ~ 1 ms. The flame reaches a height of ~ 3–4 mm. The flame glow of CO, H_2O^*, H_2^* and carbon particles with Planck spectrum

corresponding to heating to T~3000 K was identified in the spectra. With an increase in energy density to the value $H_{cr}^{(3)} > H_{cr}^{(2)}$, specific for each studied coal rank, another type of thermochemical reaction is initiated within the particle volume, which leads to the flame generated within the time interval of ~ 10 ms, ~ 3 cm high. Thermal glow with T~2000 K dominates in the spectrum.

These results allowed establishing some details of the mechanism of laser ignition of coal microparticles. Nevertheless, speaking of the possibility to use laser ignition of pulverized coal fuel, it is necessary to carry out an investigation using relatively cheap continuous semiconductor lasers.

In the present work, we describe the results of an investigation into the ignition of low-metamorphized coal ranks with the help of irradiation with continuous lasers at two wavelengths: 450 and 808 nm, and provide their interpretation from the viewpoints and ideas elaborated from the application of laser ignition.

2. Samples and experimental procedure

Low-metamorphized coal ranks were used in experiments: lignite coal from the Tisul deposit of the Kansk-Achinsk brown coal basin and high volatile C bituminous coal from the Sokolovskoye deposit. To obtain experimental samples, coal grinding was carried out in the AGO-2 ball mill, followed by wet sieving through a sieve with 63 μm mesh. The sieved powder was collected in a special vessel closed for air access. Results of the proximate analysis of coal samples are presented in Table 1.

Measurement of the size distribution of coal powder particles with the help of Fritsch Analysette 22 comfort laser diffractometer showed that coal particle size was within the range 0.5 to 63 μm. The largest number of particles is within the range of 10–40 μm, with a distribution maximum of 20 μm.

Table 1
Results of the proximate analysis
of analytical coal samples

Coal rank	Proximate analysis, %		
	W^a	A^d	V^{daf}
Lignite coal	11.1	9.5	51.1
High volatile C bituminous coal	5.7	4.7	42.6

W^a – analytical moisture, A^d – ash content, V^{daf} – parameter indicating the yield of volatile substances

Samples with the bulk density of $\rho = 0.4$ g/cm³ were used in the experiments; they were placed in a copper capsule 5 mm in diameter, 2 mm deep.

The scheme of experimental setup for measurements of the kinetic and energy characteristics of coal ignition is presented in Fig. 1.

Coal ignition was carried out with the help of semiconductor lasers (L) at the wavelength of λ = 808 nm or λ = 450 nm with controllable radiation power up to 10 W and 20 W, respectively.

Radiation power was adjusted with the help of glass neutral light filters (1) with known attenuation coefficients. To monitor the power, a portion of radiation (8%) was conducted by a transparent glass plate (2) onto calibrated photodiode (3). With the help of a focusing lens (4) with a focal distance F = 25 cm and a rotating mirror (5), the radiation was directed onto the sample (6), and placed on a massive base (7). The area of the laser spot on the sample was S = 0.03 cm². Sample glow was collected with lens (8) and recorded with the help of a photoelectron multiplier Hamamatsu H10721-20 (9) and oscillograph LeCroy WaveJet WJ332A (10). The time of laser radiation exposure was governed with the help of pulse generator G5-56 (11). Exposure time was 1 sec. The laser and oscillograph (10) sweep were launched synchronously with the help of a generator (11).

The spectral characteristics of the glow arising from coal combustion under the action of laser radiation were measured according to the scheme shown in Fig. 2.
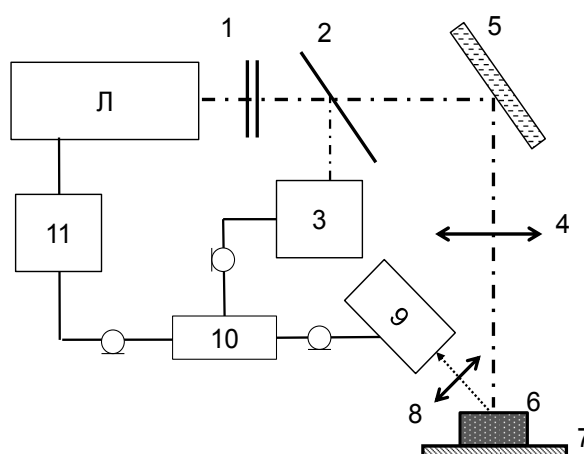

Fig. 1. Schematic of the experimental setup for measuring the kinetic and energy characteristics of coal ignition: 1 – neutral light filters; 2 – beam splitting plate; 3 – photodiode; 4 – lens F = 25 cm; 5 – rotating mirror; 6 – sample; 7 – base; 8 – lens F = 10 cm; 9 – photoelectron multiplier; 10 – oscillograph; 11 – generator G5-56, L – laser radiation source (808 nm or 450 nm).
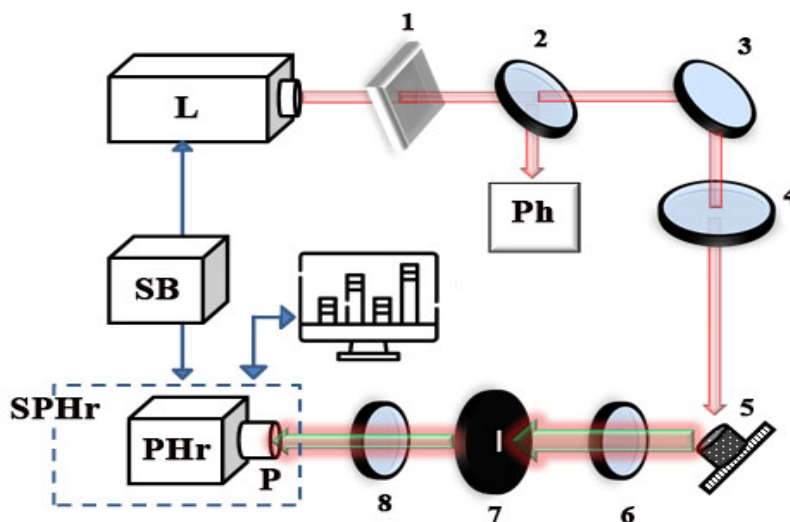
Fig. 2. Schematic of the experimental setup: 1 – neutral light filters; 2 – beam splitting plate; 3 – rotating mirror; 4 – lens (F = 25 cm); 5 – experimental assemblage with the sample; 6, 8 – lenses (F = 10 cm); 7 – spectral-temporal slit (turned at 90° in the Figure), L – laser radiation source, Ph – photodiode, PHr – photochronograph, P – polychromator, SPHr – spectrophotochronograph VZGLYAD-2A, SB – synchronization unit, C – computer.

Coal ignition was carried out with the help of single pulses of the lasers similar to those used in the scheme (Fig. 1). The radiation of the laser (L) was attenuated with neutral light filters (1). Radiation power was monitored by directing a portion of radiation (8%) with the help of a transparent glass plate (2) onto a calibrated photodiode (Ph). The radiation was directed with a rotating mirror (3) and focusing lens with the focal distance F = 25 cm (4) onto the sample (5). The holder design allowed mounting the sample (5) at an angle of 45° to the laser beam and the optical axis of the measuring system. The area of the laser spot on the sample was S = 0.03 cm^2.

The glow in the region near the sample surface was recorded using polychromator (P) and photochronograph (PHr) based on an electron-optical converter (EOC) operating in the linear sweep mode, forming an integrated spectrochronograph (SPHr). The image of the sample surface was built up with the help of lens (6) in the plane of the spectral-temporal slit (7). The hole in the slit was 0.2×0.1 mm in size and determined the spectral and temporal resolution of the recording system. The image of the spectral-temporal slit was transmitted with the help of lens (8) at a scale of 1:1 to the inlet of polychromator (P). So, the spatial resolution in the object region corresponded to slit size. Polychromator (P) decomposed the glow into the components within spectra range 350–750 nm. The time-base sweep of the spectral band was performed with the help of photochronograph (PHr). The light matrix from the output screen of EOC

was read by the CCD matrix. The signal from the CCD matrix was transmitted to the memory of a computer (C) for subsequent numerical processing. The spectral resolution was 10 nm. Sweep with the maximal duration of the streak camera 2.3 ms/screen was used in the work. The laser and streak camera sweep were started at the corresponding moments with the help of G5-56 pulse generator (SB).

The recorded signal was an array; its vertical elements allowed plotting the spectrum of sample glow within the range of 350−750 nm at a definite moment, while the horizontal elements allowed plotting glow kinetics at a chosen wavelength within the indicated spectral range.

The reference lamp method was used to correct glow spectra for the spectral sensitivity of the measuring tract [20].

3. Experimental results

Comparative investigation of the kinetic characteristics of coal particle ignition during the action of laser radiation for 1 sec at the wavelengths of 808 and 450 nm was carried out for lignite and high volatile C bituminous coal ranks. The experimental circuit presented above (Fig. 1) was used. Some oscillograms are shown in the inserts in Fig. 3 a, b. For both coal ranks, ignition starts after a definite time interval t_z. The dependence of ignition time t_z on power density W for both coal ranks under the action of the radiation with λ = 808 and 450 nm is shown in Fig. 3.
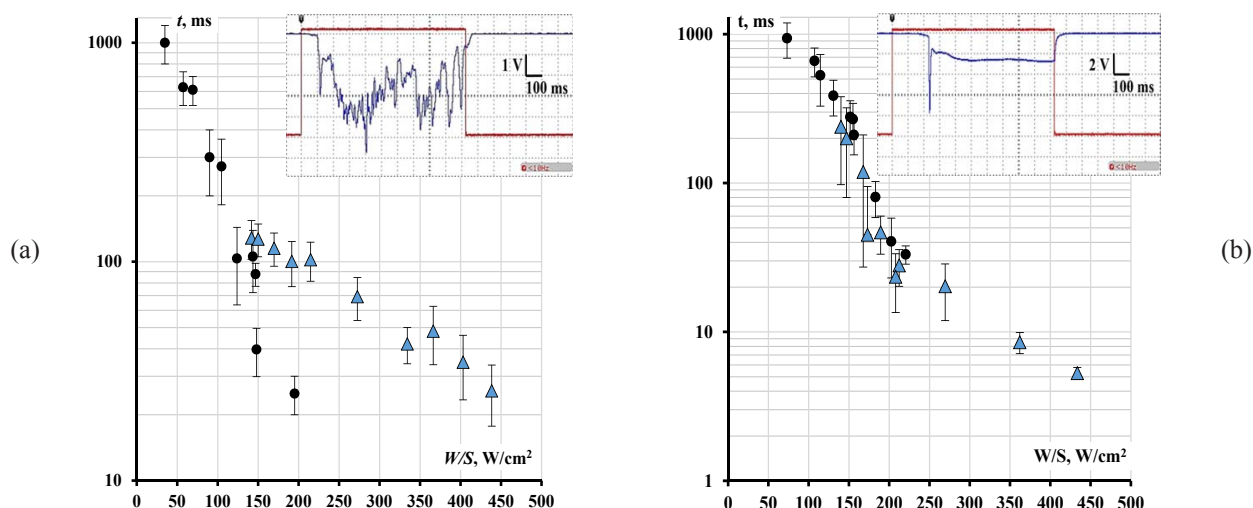
Fig. 3. Dependence of coal ignition delay time on the power density of laser radiation: (a) – lignite coal; (b) – high volatile C bituminous coal. Inserts: oscillograms of the dependence of glow intensity on time during laser action. (▲ – 450 nm, ● – 808 nm).

At low radiation power density, the time of ignition delay t_z exhibits substantial statistical scattering, which is the reason for large confidence intervals for some points (see Fig. 3). Confidence intervals were calculated using Student method for 10 measurements at the confidential probability $\alpha = 0.9$. With an increase in power density, time t_z decreases monotonously.

In the next series of experiments, we measured the probability of coal ignition depending on laser radiation power density at $\lambda = 808$ nm and $\lambda = 450$ nm. With the fixed power density, 10 samples were consequently irradiated with 1 sec pulses. The occurrence of ignition during irradiation was determined from oscillograms (see inserts in Fig. 3). The probability of ignition was determined:

$$P = n/N, \qquad (1)$$

where n is the number of ignition events during the action of laser radiation, N = 10 is the total number of experiments at a fixed power density.

To compare laser action at different wavelengths, it is of interest to determine the probability of sample ignition depending on the density of absorbed radiation power W_p. The radiation is completely absorbed by coal samples, so W_p is connected with the exposure power density W_e according to Eq. (2):

$$W_p = (1-R) \times W_e, \qquad (2)$$

where R is the reflectance coefficient of a sample of the corresponding coal rank.

Reflectance coefficients of lignite and high volatile C bituminous coal ranks were measured for radiation with $\lambda = 808$ nm and $\lambda = 450$ nm using the photometric integrating sphere, similarly to [21, 22]. Results are presented in Table 2.

The experimental values of W_e and the corresponding W_p and P, calculated from the experimental data for lignite coal rank using Eqs. (1) and (2) are presented in Table 3.

Similar measurements and calculations for coal of high volatile C bituminous coal rank are presented in Table 4.

The P(W) dependences are shown in Fig. 4 for both coal ranks. Experimental points in Fig. 4 are approximated with the error integral:

$$p(W) = \frac{1}{\sqrt{2\pi}} \int_O^W \frac{exp(W - W_{cr})}{2\Delta W} dW, \qquad (3)$$

where W_{cr} is the critical laser radiation power density corresponding to the 50% flare probability, which we accept as ignition threshold, ΔW is the mean square deviation.

Table 2
Reflectance coefficients of the experimental coal samples of lignite and high volatile C bituminous ranks for wavelengths 450 and 808 nm

	R, %	
λ, nm	Lignite coal	High volatile C bituminous coal
450	3.4	4.5
808	13.8	8.9

Table 3
Ignition probabilities for samples of lignite coal depending on the density of absorbed radiation power W_p and exposure power density W_e

	808 nm			450 nm	
W_e	W_p	P	W_e	W_p	P
200	172	1	346	334	1
172	148	1	282	273	1
166	143	0.9	222	215	0.8
144	124	0.8	198	192	0.6
126	108	0.6	176	170	0.5
104	90	0.5	154	149	0.4
80	69	0.3	147	142	0.3
35	30	0.1	133	128	0.1
20	17	0	110	106	0

Table 4
Ignition probabilities for samples of high volatile C bituminous coal depending on the density of absorbed radiation power W_p and exposure power density W_e

	808 nm			450 nm	
W_e	W_p	P	W_e	W_p	P
200	182	1	282	269	1
185	168	1	222	212	1
134	122	0.8	195	186	0.9
126	114	0.6	180	172	0.8
109	100	0.4	175	168	0.5
100	91	0.2	155	148	0.2
80	73	0	133	127	0
35	32	0	110	105	0

Continuous curves (Fig. 4) relate to the $P(W_e)$ dependence, dash curves relate to the $P(W_p)$ dependence. Ignition parameters W_{cr} and ΔW, determined for the $P(W_p)$ dependence, are shown in Table 5.
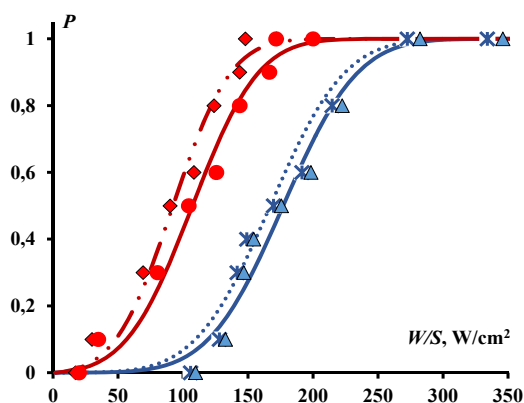
In the next series of experiments, we measured the spectra of near-surface glow arising during coal ignition, using the scheme of the experiment presented in Fig. 2.

The laser with radiation at a wavelength of 808 nm was used in these experiments. The application of the laser at the wavelength of 450 nm turned out to be impossible because this wavelength coincides with the maximum of the spectral sensitivity of photocathode in EOC of photochronograph, and even a small portion of scattered radiation caused blinding of EOC and made measurements impossible.

A photochronograph sweep with a maximal duration 2.3 ms per screen was used in the experiments. Within the framework of the temporal scale of this experiment, this sweep was practically instantaneous, and this excluded the possibility to carry out kinetic measurements. The spectra were measured with different delays from the start of the photochronograph sweep to the start of a laser pulse.

Table 5
The critical power density of laser radiation (W_{cr}) corresponding to the 50% probability of flare, determined for the dependence $P(W_p)$ of lignite and high volatile C bituminous rank coal samples at the wavelengths of 450 and 808 nm

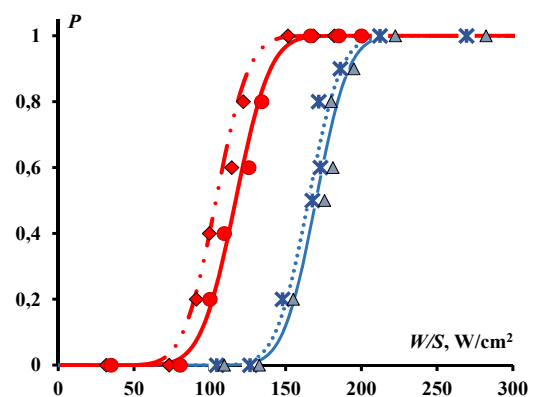|	Lignite coal		High volatile C bituminous coal	
λ	W_{cr}, W/cm^2	ΔW, W/cm^2	W_{cr}, W/cm^2	ΔW, W/cm^2
450	165	45	165	17
808	90	35	100	20

Fig. 4. Probability of coal ignition depending on the power density of laser radiation: (a) – lignite coal; (b) – high volatile C bituminous coal. (λ = 450 nm: ▲ – without taking reflectance into account; ✶ – taking reflectance into account; λ = 808 nm; ● – without taking reflectance into account; ♦ – taking reflectance into account).
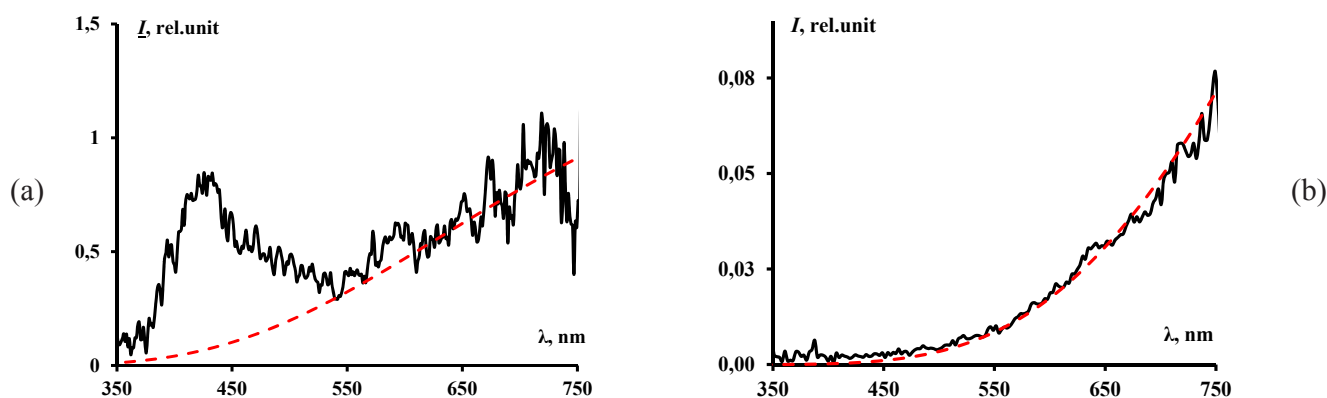
Fig. 5. Glow spectra of the lignite coal during the action of laser pulse at different moments of time after switching the radiation on (a) t = 100 ms (dash curve, approximation with Planck formula at T = 2700 K), (b) t = 500 ms (dash curve, approximation with Planck formula at T = 1900 K).
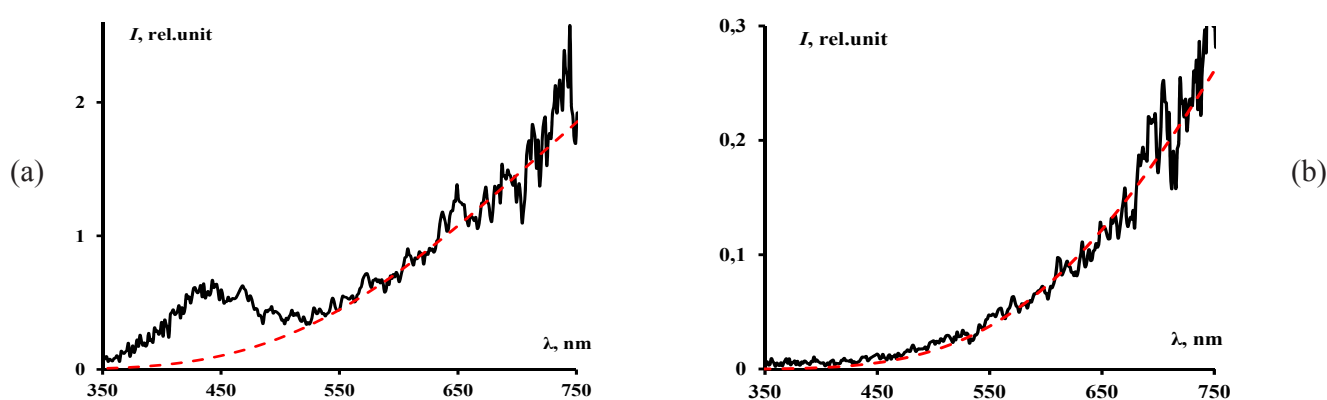

Fig. 6. Glow spectra of the high volatile C bituminous coal during the action of laser pulse at different moments of time after switching the radiation on (a) t = 50 ms (dash curve, approximation with Planck formula at T = 2350 K), (b) t = 200 ms (dash curve, approximation with Planck formula at T = 2000 K).

Similarly to previous measurements, the duration of laser pulse affecting coal samples was τ_i = 1 sec, and power density was P = 200 W/cm².

Glow spectra of lignite coal at the moment 100 ms and 500 ms after laser switching are presented in Fig. 5.

Similar measurements were carried out using coal of high volatile C bituminous rank. Spectra measured at the time moments 50 ms and 200 ms after laser switching on is presented in Fig. 6.

4. Discussion

One can see in the oscillograms (see insert in Fig. 3) that after ignition delay t_z combustion proceeds till radiation is over and stops simultaneously with radiation. Therefore, under our experimental conditions, there is no transition to stationary combustion. This is true for the whole power density range involved in the studies for both coal ranks. The possibility of transition to the steady combustion mode for exposure to laser radiation for 1 and 2 min was tested. In all cases, combustion ceases after the laser is switched off, or after the sample is completely burnt out in the irradiated zone. So, in this experimental arrangement, one cannot achieve a transition to steady combustion, which is important for practical applications. It appears that another approach is to be used to solve this problem with experiment arrangement. For instance, airflow is to be passed through pulverized coal fuel. This will enhance the access of oxygen to coal particles and will provide better combustion conditions.

The time of ignition delay t_z for lignite coal at the same power density W is shorter for 808 nm radiation than for 450 nm radiation (see Fig. 3). The situation is quite contrary for high volatile C bituminous coal: the time of ignition delay t_z is somewhat shorter for 450 nm radiation than for 808 nm. It is difficult to interpret this result at present. A possible reason may be in the features of

the structure of brown and black coal. It will be necessary to return to this interpretation after similar measurements with other ranks of black coal in the metamorphism series.

Now the density of absorbed energy E_n consumed for coal ignition with the probability $P = 0.5$ for both kinds of radiation will be evaluated.

This value may be determined using the equation:

$$E_n = W_{ck} \times t_{0.5} \qquad (4)$$

where $t_{0.5}$ is delay time for ignition probability 0.5.

The value of $t_{0.5}$ will be determined from Fig. 3: $\lambda = 808$ nm $t_{0.5} \approx 0.3$ sec and 0.5 sec for lignite and high volatile C bituminous rank coal, respectively $\lambda = 450$ nm $t_{0.5} \approx 0.11$ s and 0.08 s for lignite and high volatile C bituminous rank coal, respectively.

The values of W_{cr} will be taken from Table 5.

As a result of calculations taking into account measurement errors, energy consumption E_n for ignition of the studied coal ranks will be:

For radiation with $\lambda = 450$ nm, we obtain $E_n \approx 18$ J/cm² for coal of lignite, and $E_n \approx 13$ J/cm² for high volatile C bituminous coal. For radiation with $\lambda = 808$ nm, $E_n \approx 27$ J/cm² for coal of rank lignite, and $E_n \approx 50$ J/cm² for high volatile C bituminous coal.

The above-presented estimated energy consumption for ignition of the studied coal ranks allows us to conclude that the use of radiation with $\lambda = 450$ nm is more economical.

It follows from the results presented in Fig. 4 and Table 5 that ignition of both coal ranks occurs for the blue radiation ($\lambda = 450$ nm) at higher power densities of absorbed energy W_p than for red radiation ($\lambda = 808$ nm). This result is to be considered in more detail.

The W_p value may be represented as

$$W_p = n \times E_f = n \times (h \times c / \lambda) \qquad (5)$$

where n is the number of absorbed quanta of radiation per unit area and unit time, E_f is photon energy.

For the blue ($\lambda_b = 450$ nm) and red ($\lambda_r = 808$ nm) radiation, respectively, we may write:

$$W^{(b)} = n_b \times (h \times c / \lambda_b)$$
$$W^{(r)} = n_r \times (h \times c / \lambda_r) \qquad (6)$$

Therefore,

$$W^{(b)} / W^{(r)} = (n_b \times \lambda_r) / (n_r \times \lambda_b) = 1.8 \times n_b / n_r \qquad (7)$$

We use (7) for the critical densities of radiation power presented in Table 5:

for lignite coal grade – $W^{(b)}_{cr} / W^{(r)}_{cr} = 1.83$ taking into account (7) – $n_b / n_r = 1.02$ for high volatile C bituminous coal grade – $W^{(b)}_{cr} / W^{(r)}_{cr} = 1.65$ taking into account (7) – $n_b / n_r = 0.92$.

If the mean square deviation is taken into account for W_{cr} determination, it is possible to accept $n_b \approx n_r$ within the measurement error limits.

It follows from these results that the number of quanta of energy absorbed per unit time by the corresponding coal rank is equal for blue and red radiation. The difference in the energy thresholds of ignition is connected with the difference in the energy of radiation quanta of different wavelengths.

The latter result allows assuming that laser energy is absorbed in the form of photons, that is, the quantum nature of light manifests itself.

Absorption of light causes the formation of excited states in coal macromolecules or the rupture of some chemical bonds. As a result of the de-excitation of these states, energy passes into heat and causes the heating of coal particles. At W_{cr}, the temperature of coal particles is sufficient for their ignition.

It follows from the oscillograms of coal glow presented in the inserts (see Fig. 3) that the first glow maximum appears after ignition delay time t_z. This allows us to assume that the ignition process at the initial moment has some specific features distinguishing it from the process at subsequent moments.

Measuring glow spectra taking into consideration the statistical nature of the time of ignition delay t_z, we recorded the glow at the first peak, which is seen in the oscillograms (see Fig. 3) and glow at subsequent stages of combustion during irradiation. The glow spectra that correspond to the first peak in the oscillograms are shown in Figs. 5a and 6a (see Fig. 3). Two components may be distinguished in the spectra: the first one is glowing within the range of 350–550 nm with the maximum at $\lambda \sim 430$–450 nm, and the second is thermal glow, with the spectrum described by Planck formula ($T = 2700$ K for lignite coal and $T = 2400$ K for high volatile C bituminous coal). Taking into account spectral-kinetic measurements under pulsed action in our previous works [12], we may relate the first spectral component to the glow of CO (CO_2^*) flame, while the second one may be assigned to the glow of either

particle surface or heated carbon particles flying away. The general view of the spectrum is similar to that observed by us previously under the pulsed action [12, 15]. This allows us to conclude that the glow is connected with chemical reactions initiated in the volume of coal particles, leading to the emergence and ignition of volatile substances, similar to the case of pulsed irradiation at the second stage of ignition for energy density $H_{cr}^{(2)}$ [15]. The glow spectra at the subsequent moment (Figs. 5b and 6b) are described by Planck formula (T ≈ 1900 K for lignite coal and T ≈ 2000 K for high volatile C bituminous coal) and are connected with the ignition of non-volatile residue and the release of heated carbon particles, similarly to the case of pulsed irradiation at the third stage of ignition for energy density $H_{cr}^{(3)}$ [14, 16].

5. Conclusions

1. Ignition of the microparticles of low-metamorphized coal ranks lignite and high volatile C bituminous by the radiation of semiconductor lasers at the wavelengths of 450 and 808 nm with 1 sec exposure occurs only during the action of radiation. There is no transition to steady combustion.

2. The time of ignition delay depends on the power density of laser radiation W and decreases monotonously with an increase in W.

3. For laser ignition of lignite and high volatile C bituminous coal ranks, energy consumption is lower for radiation with λ = 450 nm than for λ = 808 nmm.

4. Analysis of the results obtained in the measurement of threshold values of the absorbed power of laser radiation with wavelengths 450 and 808 nm for coal of lignite and high volatile C bituminous ranks allows assuming that absorption of the radiation has a quantum nature.

5. Two components contribute to the glow spectra of coal particles measured at the initial stage of ignition: the flame of CO (CO_2*) and thermal glow connected with carbon particles flying out, heated to T>2000 K for both coal ranks. Only the glow of heated carbon particles with the thermal spectrum with T~2000 K is observed in the spectra at subsequent stages.

Acknowledgments

References

[1]. L.D. Paul, R.R. Seeley, *Corrosion* 47 (1991) 152–159. DOI: 10.5006/1.3585231

[2]. A.S. Askarova, E.I. Karpenko, Y.I. Lavrishcheva, V.E. Messerle, A.B. Ustimenko, *IEEE Plasma Sci.* 35 (2007) 1607. DOI: 10.1109/TPS.2007.910142

[3]. V.E. Messerle, E.I. Karpenko, A.B. Ustimenko, O.A. Lavrichshev, *Fuel Process. Technol.* 107 (2013) 93–98. DOI: 10.1016/j.fuproc.2012.07.001

[4]. J.C. Chen, M. Taniguchi, K. Narato, K. Ito, *Combust. Flame* 97 (1994) 107–117. DOI: 10.1016/0010-2180(94)90119-8

[5]. A.F. Glova, A.Ju Lysikov, M.M. Zverev, *Quantum Electron.* 39 (2009) 537–540. DOI: 10.1070/QE2009v039n06ABEH013906

[6]. M. Taniguchi, H. Kobayashi, K. Kiyama, Y. Shimogori, *Fuel* 88 (2009) 1478–1484. DOI: 10.1016/j.fuel.2009.02.009

[7]. V.M. Boiko, P. Volan'skii, V.F. Klimkin, *Combust. Explos. Shock Waves* 17 (1981) 545–549. DOI: 10.1007/BF00798143

[8]. T.X. Phuoc, M.P. Mathur, J.M. Ekmann, *Combust. Flame* 93 (1993) 19–30. DOI: 10.1016/0010-2180(93)90081-D

[9]. A.V. Kuzikovskii, V.A. Pogodaev, *Combust. Explos. Shock Waves* 13 (1977) 666–669. DOI: 10.1007/BF00742231

[10]. T.X. Phuoc, M.P. Mathur, J.M. Ekmann, *Combust. Flame* 94 (1993) 349–362. DOI: 10.1016/0010-2180(93)90119-N

[11]. B.P. Aduev, D.R. Nurmukhametov, N.V. Nelyubina, R.Y. Kovalev, A.N. Zaostrovskii, Z.R. Ismagilov, *Russ. J. Phys. Chem. B* 10 (2016) 963–965. DOI: 10.1134/S1990793116060154

[12]. B.P. Aduev, D.R. Nurmukhametov, R.Y. Kovalev, Ya.V. Kraft, A.N. Zaostrovskii, Z.R. Ismagilov, A.V. Gudilin, *Opt. Spectrosc.* 125 (2018) 293–299. DOI: 10.1134/S0030400X18080039

[13]. B.P. Aduev, Y.V. Kraft, D.R. Nurmukhametov, Z.R. Ismagilov, *Chem. Sustain. Dev.* 27 (2019) 549–555. DOI: 10.15372/CSD2019172

[14]. B.P. Aduev, D.R. Nurmuhametov, Y.V. Kraft, Z.R. Ismagilov, *Chem. Sustain. Dev.* 28 (2020) 518–526. DOI: 10.15372/CSD2020260

[15]. B.P. Aduev, D.R. Nurmukhametov, Y.V. Kraft, Z.R. Ismagilov, *Opt. Spectrosc.* 128 (2020) 2008–2014. DOI: 10.1134/S0030400X20120838

[16]. B.P. Aduev, D.R. Nurmukhametov, Y.V. Kraft, Z.R. Ismagilov, *Opt. Spectrosc.* 128 (2020) 429–435. DOI: 10.1134/S0030400X20030029

[17]. B.P. Aduev, D.R. Nurmukhametov, Ya.V. Kraft, Z.R. Ismagilov, *Opt. Spectrosc.* 130 (2022) 35–42. DOI: 10.21883/OS.2022.08.52905.3750-22

[18]. B.P. Aduev, D.R. Nurmukhametov, Ya.V. Kraft, Z.R. Ismagilov, *Russ. Phys. Chem. B* 16 (2022) 227–235. DOI: 10.31857/S0207401X22030025

[19]. B.P. Aduev, D.R. Nurmukhametov, N.V. Nelyubina, Y.V. Kraft, Z.R. Ismagilov, *J. Appl. Spectrosc.* 88 (2021) 761–764. DOI: 10.1007/s10812-021-01237-w

[20]. L.V. Levshin, A.M. Saletsky. Luminescence and its measurements Molecular luminescence Moscow, MSU, 1989, p. 272.

[21]. B.P. Aduev, D.R. Nurmukhametov, G.M. Belokurov, A.A. Zvekov, A.P. Nikitin, I.Y. Liskov, A.V. Kalenskii, *Tech. Phys.* 59 (2014) 1387–1392. DOI: 10.1134/S1063784214090023

[22]. B.P. Aduev, D.R. Nurmukhametov, A.A. Zvekov, A.P. Nikitin, N.V. Nelyubina, G.M. Belokurov, A.V. Kalenskii, *Instrum. Exp. Tech.* 58 (2015) 765–770. DOI: 10.1134/S0020441215050012